Geochemical Cycles in Sediments Deposited on the Slopes of the Guaymas and Carmen Basins of the Gulf of California Over the Last 180 Years

Walter E. Dean
U.S. Geological Survey, Denver, CO, dean@usgs.gov

Carol Prideb
Marine Science Program, Savannah State University, Savannah, GA 31404, USA

Robert Thunell
Department of Geological Sciences, University of South Carolina, Columbia, SC 29208, USA

ELSEVIER

Quaternary Science Reviews 23 (2004) 1817–1833

QSR

Geochemical cycles in sediments deposited on the slopes of the Guaymas and Carmen Basins of the Gulf of California over the last 180 years

Walter Dean[a,*], Carol Pride[b], Robert Thunell[c]

[a] US Geological Survey, MS 980 Federal Center, PO Box 25046, Denver, CO 80225, USA
[b] Marine Science Program, Savannah State University, Savannah, GA 31404, USA
[c] Department of Geological Sciences, University of South Carolina, Columbia, SC 29208, USA

Received 10 November 2003; accepted 11 March 2004

Abstract

Sediments deposited on the slopes of the Guaymas and Carmen Basins in the central Gulf of California were recovered in two box cores. Q-mode factor analyses identified detrital-clastic, carbonate, and redox associations in the elemental composition of these sediments. The detrital-clastic fraction appears to contain two source components, a more mafic component presumably derived from the Sierra Madre Occidental along the west coast of Mexico, and a more felsic component most likely derived from sedimentary rocks (mostly sandstones) of the Colorado Plateau and delivered by the Colorado River. The sediments also contain significant siliceous biogenic components and minor calcareous biogenic components, but those components were not quantified in this study. Redox associations were identified in both cores based on relatively high concentrations of molybdenum, which is indicative of deposition under conditions of sulfate reduction. Decreases in concentrations of molybdenum in younger sediments suggest that the bottom waters of the Gulf have became more oxygenated over the last 100 years. Many geochemical components in both box cores exhibit distinct cyclicity with periodicities of 10–20 years. The most striking are 20-year cycles in the more mafic components (e.g., titanium), particularly in sediments deposited during the 19th century. In that century, the titanium cycles are in very good agreement with warm phases of the Pacific Decadal Oscillation, implying that at times of greater influx of titanium-rich volcanic debris, there were more El Niños and higher winter precipitation. The cycles are interpreted as due to greater and lesser riverine influx of volcanic rock debris from the Sierra Madre. There is also spectral evidence for periodicities of 4–8 and 8–16 years, suggesting that the delivery of detrital-clastic material is responding to some multiannual (ENSO?) forcing.
Published by Elsevier Ltd.

1. Introduction and background

The Gulf of California is an actively growing ocean basin, created over the last four million years by seafloor spreading (Moore, 1973). The Guaymas and Carmen Basins are two deep, semi-enclosed basins that formed as a result of this spreading (Fig. 1). There are several potential sediment sources to the Gulf of California. Five major rivers drain the volcanic rocks of the west slope of the Sierra Madre Occidental: Rios Sonora, Matape, Yaqui, Mayo, and Fuerte (Fig. 1). However, today much of the sediment in these rivers is trapped in dams built along the rivers since 1940 (Baumgartner et al., 1991). The lower Colorado River drains sedimentary rocks of the Colorado Plateau, but today much of its sediment load also is deposited behind dams in Lake Powell and Lake Mead. Based on Q-mode factor analysis of major-element contents of bulk sediment from 87 localities throughout the Gulf, Baba et al. (1991a) identified a terrigenous factor that accounts for 80–90% of the total sedimentation along the eastern margin of the central and southern Gulf. Baba et al. (1991a) also analyzed the mineralogy of samples from the Colorado River and coastal rivers of Mexico. Samples from the northern drainages had the highest quartz/feldspar ratios reflecting sedimentary, plutonic, and metamorphic sources. Sediments from

*Corresponding author. Tel.: +1-303-236-5760; fax: +1-303-236-5349.
E-mail address: dean@usgs.gov (W. Dean).

0277-3791/$ - see front matter Published by Elsevier Ltd.
doi:10.1016/j.quascirev.2004.03.010

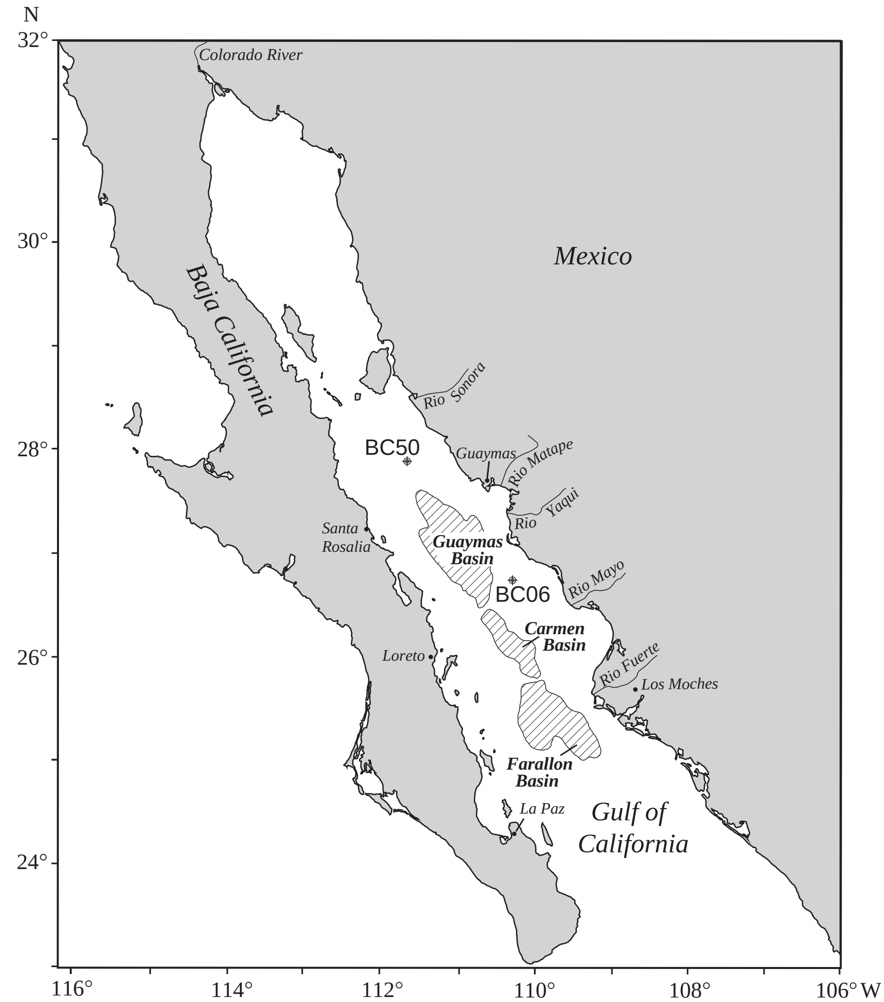

Fig. 1. Map of western Mexico, the Gulf of California, and Baja California showing locations of cores described in this paper. Enclosed basins of the central Gulf are shown by the diagonally lines areas.

rivers draining the Sierra Madre into the central Gulf had the lowest quartz/feldspar ratios reflecting volcanic sources. Fine-grained terrigenous sediments from the Colorado River are mainly confined to the northern Gulf and do not appear to be escaping in significant amounts to the central Gulf region. The Baja California peninsula is low lying with few rivers and is not considered to be a major sediment source (Baba et al., 1991a).

The Gulf of California is characterized by marked seasonal changes in circulation and productivity driven by changes in atmospheric circulation over the eastern North Pacific and the adjacent North American continent. Winter conditions are characterized by strong northwesterly winds that transport water out of the Gulf, and produce upwelling and associated high organic productivity (Thunell et al., 1994; Thunell, 1998). During the winter, the subtropical North Pacific high-pressure cell is at its most southerly position, and circulation over the eastern North Pacific is dominated by a succession of Aleutian lows (Fig. 2A). A high-pressure cell is established during most of the winter months over the Great Basin of western United States, and a low-pressure cell dominates over western Mexico (Fig. 2A).

During the summer, the subtropical high moves northward and dominates over the eastern North Pacific. Circulation around the subtropical high strengthens the California Current producing strong upwelling along the California margin (Fig. 2B). However, the low-pressure cell that is established over Arizona during the summer drives the southwestern monsoon, and produces weak southerly winds over the Gulf. Surface waters flow into the Gulf from the Pacific at this time including Tropical Surface Water and Subtropical Subsurface Water (Bray, 1988). Below these seasonally varying surface-water masses is oxygen-deficient North Pacific Intermediate Water which currently establishes an oxygen minimum zone (OMZ) between 500 and 1000 m (Bray, 1988; Thunell, 1998). Summer is also the rainy season and organic productivity in the Gulf is low. Maximum precipitation (average

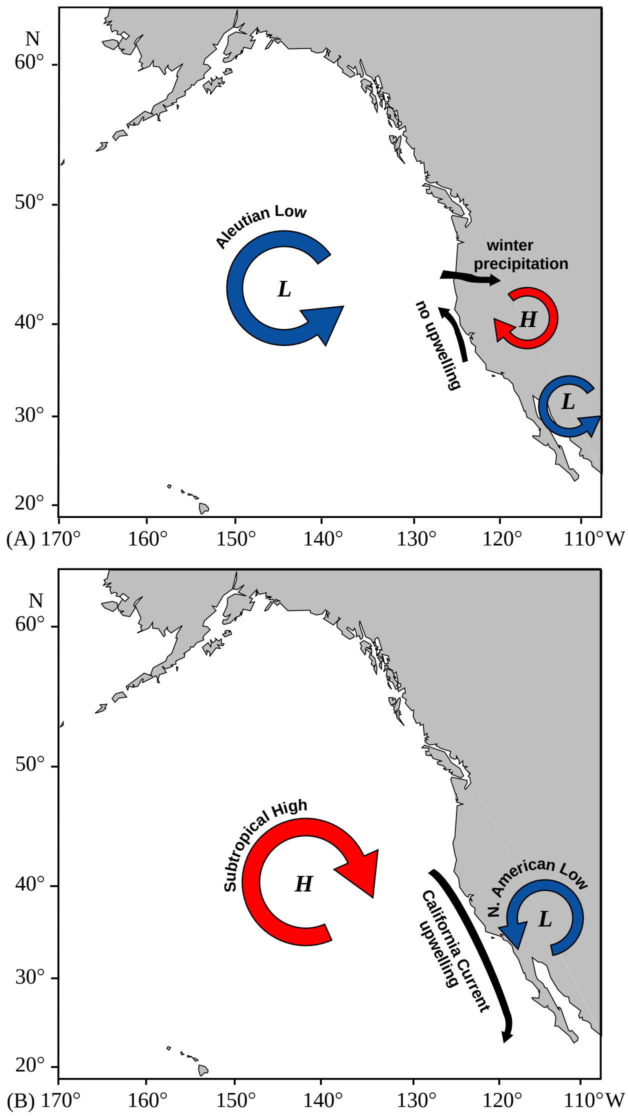

Fig. 2. (A) Generalized winter atmospheric circulation over western North America and the northeast Pacific Ocean that results in no California Current upwelling, abundant precipitation over the western United States, and export of water from the Gulf of California. (B) Generalized summer atmospheric circulation over western North America and the northeast Pacific Ocean that results in strong upwelling associated with the California Current, monsoonal precipitation over the southwestern United States and northwestern Mexico, and transport of North Pacific water into the Gulf of California.

of 70% of annual) usually occurs in August and September. A comparable high percentage of discharge of the three main rivers draining into the central Gulf (Rios Yaqui, Mayo, and Fuerte; Fig. 1) occurs during this 3-month period (Baumgartner et al., 1991).

The strong seasonality of rainfall and river discharge to the central Gulf should have a profound effect on sedimentation there. There should also be considerable variation in sedimentation driven by interannual and decadal events such as El Niños, La Niñas, and the Pacific Decadal Oscillation (PDO). Seasonal variations are obvious in sediments within the OMZ, which are characterized by seasonal laminations (varves; Calvert, 1966; Baumgartner et al., 1991). The light-colored laminae consist mainly of diatom-rich biogenic sediment deposited from late fall to spring (Calvert, 1966; Baumgartner et al., 1991; Thunell, 1998). Using back-scattered electron imagery (BSEI), Pike and Kemp (1997) have detected sublaminae within the light-colored laminae that contain distinct diatom species/assemblages. The dark laminae contain more detrital-clastic material, and represent predominantly summer deposition. Calvert (1966) concluded that the terrigenous material is brought in by rivers during torrential summer rains. Baumgartner et al. (1991) suggested that the terrigenous material is mainly eolian, brought in during strong convective summer thunder storms, because they could not find a difference in mass accumulation rate (MAR) of terrigenous material before and after dam construction began in 1940.

Geochemical data are presented here on sediments from two box cores sampled at 0.5-cm intervals. Cores BC06 and BC50 are part of a series of box, gravity, and piston cores collected in July, 1990 on R./V. *Atlantis II* cruise 125/8. Both cores were sampled at 0.5-cm intervals for geochemical analyses. Core BC06 was collected on the slope between the Guaymas and the Carmen Basins close to the west coast of mainland Mexico between Rio Yaqui and Rio Mayo (26°49.39′N, 110°13.78′ W; water depth = 754 m; Fig. 1). This core has a constant sedimentation rate of 2.6 mm/yr determined by ^{210}Pb dating (Thunell et al., 1994). Therefore, each sample represents an average of 1.9 years. Core BC50 was collected farther north than BC06 on the northern slope of Guaymas Basin (27°47.15′ N, 111°42.51′ W; water depth = 745 m; Fig. 1). This site is more distant from either shoreline than that of BC06. The linear ^{210}Pb sedimentation rate in core BC50 is 1.8 mm/yr (Thunell et al., 1994), and each sample represents an average of 2.7 years.

The main purpose of this investigation was to determine if different sediment sources could be identified by geochemical signatures, and if these sources changed over the last 200 years, particularly in response to dam building in the 20th century. Secondary objectives were to determine if there were any geochemical signatures of past organic productivity and changes in redox conditions in these anoxic basins. Because of the strong seasonality of precipitation in the Gulf, a third objective was to detect any interannual to decadal variability in climate.

2. Methods

The sediment samples were analyzed for 40 major, minor, and trace elements by inductively coupled

plasma–atomic emission spectrometry in USGS laboratories in Denver (ICP-AES; Briggs, 2002). Concentrations of 28 elements (Al, Ca, Fe, K, Mg, Na, P, Ti, Mn, Ba, Ce, Co, Cr, Cu, Ga, La, Li, Mo, Nb, Nd, Ni, Pb, Sc, Sr, Th, V, Y, and Zn) were above detection limits in all samples. The one exception was Mo, which was below detection limits (2 ppm) in 22 samples from the upper part of BC06. These samples were assigned a nominal value of 1 ppm Mo. Rock standards (USGS) were included with the sediment samples, and 10% of the samples were duplicated. Samples for organic carbon (C_{org}) and nitrogen analyses were acidified with H_3PO_4 to remove $CaCO_3$ and then analyzed with a Perkin-Elmer 2400 CHN analyzer at the University of South Carolina. The biogenic silica content of samples was determined by the Na_2CO_3 extraction method described by Mortlock and Froelich (1989). Biogenic silica was converted to percent opal ($SiO_2 \cdot nH_2O$) by multiplying the measured percentage of biogenic silica by 2.4. Isotope ratios of total N and C_{org} ($^{15}N/^{14}N$ and $^{13}C_{org}/^{12}C_{org}$) were determined at the University of South Carolina on a VG OPTIMA stable–isotope-ratio mass spectrometer linked to a Carlo Erba Elemental Analyzer. Nitrogen–isotope ratios are reported in the usual per mil delta notation relative to air ($\delta^{15}N$, ‰). Samples for $\delta^{13}C_{org}$ analyses were acidified prior to analyses to remove any $CaCO_3$. Organic-carbon–isotope ratios are reported in the usual per mil delta notation relative to the Vienna Pee Dee belemnite carbonate standard ($\delta^{13}C_{org}$, ‰; VPDB).

Sedimentation rates were determined by the ^{210}Pb dating method described by Kuehl et al. (1993), and results for these two box cores are described in Thunell et al. (1994). The slopes of the excess ^{210}P versus depths curves are linear for both cores. We assume, therefore, that the sedimentation rate was more or less constant over the entire depth range in both cores. The bulk-sediment MARs (in g/cm^2/yr) were calculated by multiplying the sedimentation rate (cm/yr) by the measured dry bulk density (g/cm^3).

The geochemical data described in this paper are available in digital form at the World Data Center-A for Paleoclimatology, NOAA/NGDC 325 Broadway, Boulder, CO 80303 (phone: 303-497-6280; fax: 303-497-6513), or on the Internet at http://www.ngdc.noaa.gov/paleo/contribseries.search and search for contributor Dean, Walter E.

3. Results

Summary statistics of elemental analyses of samples from cores BC06 and BC50 are given in Tables 1 and 2. Values for average mafic and felsic igneous rocks (Krauskopf, 1967; Parker, 1967) also are given for comparison. Based on the calcium values, sediments in both cores are low in $CaCO_3$. Assuming that the detrital-clastic material in each core has the same Ca/Al as upper continental crust (UCC; 0.366; Wedepohl, 1995), then the average detrital calcium contents in BC06 and BC50 are 0.9% and 1.3% (Tables 1 and 2). If all of that the excess calcium (total minus detrital) is in $CaCO_3$, then the average $CaCO_3$ contents in cores BC06 and BC50 are 3.7% and 5.4%. Total organic matter content, as determined by loss on ignition at 550°C in marine sediments usually is about twice the total organic carbon content (W. Dean, unpublished data). Therefore, the average organic matter contents in BC06 and BC50 are 5.7% and 7.6%. This suggests that core BC50 from the northern slope of the Guaymas Basin contains slightly more organic matter and $CaCO_3$ than core BC06 from the continental slope of the Mexican mainland.

The most striking difference between the two cores is the much higher average Al content in sediments in BC06, suggesting that BC06 contains a larger detrital aluminosilicate fraction. A simple calculation assuming that the detrital material entering both basins has the same aluminum concentration as UCC (7.7%), then the average detrital fraction in BC06 is 89% and that in BC50 is 48%. This difference cannot be explained entirely by the slightly higher contents of organic matter and $CaCO_3$ in BC50, and must be due to the higher biogenic opal (biopal) content in sediments in BC50. This is confirmed by the fact that the average biopal content in samples from the top 25 cm of BC50 is 30.9% (Table 2), and that in samples from the top 25 cm of BC06 is 9.6% (Table 1).

The sediments in BC06 appear to be slightly more enriched in most major elements relative to those in BC50. However, BC50 contains considerably more biopal than BC06 (Tables 1 and 2). Therefore, in order to compare detrital components between cores, it is necessary to compute element concentrations on a nonbiogenic basis, i.e., without the diluting influences of organic matter, biopal, and $CaCO_3$ (Tables 1 and 2).

4. Discussion

4.1. Element associations: Q-mode factor analysis

In order to determine which major and trace elements are associated with which sediment components in BC06 and BC50, multivariate analyses of the inorganic geochemical data were carried out for each core by Q-mode factor analysis. In addition, the Q-mode analysis objectively determines the stratigraphic groupings of samples within each of the cores based on geochemical similarities. The computer program used is a modified version of the extended CABFAC program described by Klovan and Miesch (1976).

Table 1
Summary statistics of elemental contents of samples from core BC06 as well as World average concentrations in mafic and felsic igneous rocks (Krauskopf, 1967; Parker, 1967)

Element	Mean	Standard deviation	Minimum	Maximum	Nonbiogenic[a]	Average mafic	Average felsic
% Al	6.89	0.25	6.3	7.3	8.75	8.8	7.7
% Ca	2.39	0.74	1.3	4		6.7	4.7
% Fe	3.13	0.12	2.8	3.4	3.98	9.7	5.9
% K	2.08	0.08	1.9	2.3	2.64	0.8	3.3
% Mg[b]	1.72	0.04	1.6	1.8	2.18	4.4	1.35
% Na[b]	3.81	0.30	3.1	4.6	4.84	1.9	2.8
% P	0.13	0.04	0.11	0.47	0.16	0.14	0.07
% Ti	0.35	0.02	0.3	0.4	0.45	0.9	0.23
% Mn	0.033	0.002	0.028	0.036	0.04	0.2	0.06
ppm Ba	531	16	480	580	674	300	830
ppm Ce	45	2	39	51	57	48	100
ppm Cr	55	2	49	60	70	200	25
ppm Cu	25	2	22	32	32	100	20
ppm Co	11	1	9	12	14	45	5
ppm Ga	16	1	14	18	21	17	20
ppm La	24	1	21	27	30	39	55
ppm Li	61	2	56	66	78	15	40
ppm Mo	3	2	1	7	4	2	1.4
ppm Nb	9	1	7	10	11	20	24
ppm Nd	22	1	18	26	28	20	46
ppm Ni	31	3	28	54	40	160	8
ppm Pb	19	12	7	120	24	8	20
ppm Sc	12	0	10	13	15	24	3
ppm Sr	286	38	220	370	363	440	300
ppm Th	7	1	5	9	8	4	18
ppm V	94	5	81	100	119	200	40
ppm Y	17	1	15	18	21	25	42
ppm Zn	97	4	87	110	123	105	50
% C_{org}	2.84	0.44	1.64	4.34			
% N	0.35	0.066	0.2	0.56			
C/N	8.15	0.69	6.023	9.914			
% biopal[c]	9.56	2.2	6.02	10.95			

[a] Nonbiogenic—see text for method of calculation.
[b] Includes Na and Mg from interstitial sea salts because samples were not washed prior to drying.
[c] Top 25 cm only.

All samples were used for the Q-mode factor analysis, but before running the analyses, geochemical concentrations in percent or parts per million were scaled to be a fraction of each variable's range for each core because of the widely differing values, ranging from fractions of a percent to thousands of parts per million. The scaled values, therefore, all ranged from 0 to 1. Four-factor models explained most of the variance in both data sets. The factor analyses essentially reduced 28 geochemical variables into four composite geochemical variables, the factor loadings. To determine which geochemical variables had the most influence in each factor, the factor loadings (composite variables) were correlated with the concentration of each measured geochemical variable. The results of this correlation analysis for BC06 are given as correlation coefficients in Table 3, and for BC50 in Table 4.

4.1.1. BC06

Table 3 shows that Ti, Y, Mn, Sr, Nb, Al, and Fe, in order of decreasing correlation coefficient with factor 1 loadings, had the most influence in grouping samples in BC06 into factor 1. The sediment component responsible for the factor 1 element association is a detrital-clastic fraction, probably mafic volcanic debris from the Sierra Madre because of the high concentrations of Ti, Mn, and Fe (Table 1). Factor 3 also appears to be a more detrital-clastic association with Li, Ce, K, Al, La, and Ga, in order of decreasing correlation coefficient with factor 3 loadings (Table 3), having the most influence on grouping samples into factor 3. The high concentrations of Li, K, and Ce in factor 3 sediments suggests that they may have been derived from a more felsic source (Table 1) than factor 1 sediments, most likely brought in by the Colorado River. Fig. 4A shows that stratigraphic variations in factor 1 loadings are very similar to those of Ti concentration, and those of factor 3 are similar to variations in Li concentration. The contributions of both factors 1 and 3 detrital components varied considerably prior to about 100 years ago. The relative

Table 2
Summary statistics of elemental contents of samples from core BC50 as well as World average concentrations in mafic and felsic igneous rocks (Krauskopf, 1967; Parker, 1967)

Element	Mean	Standard deviation	Minimum	Maximum	Nonbiogenic[a]	Average mafic	Average felsic
% Al	3.68	0.37	2.8	4.2	7.96	8.8	7.7
% Ca	3.48	0.98	1.4	5.7		6.7	4.7
% Fe	1.64	0.14	1.3	1.8	3.41	9.9	5.9
% K	1.35	0.12	1.1	1.5	2.84	0.8	3.3
% Mg[b]	1.53	0.09	1.3	1.7	3.22	4.4	0.6
% Na[b]	5.57	0.43	4.8	6.4	12.13	0.96	2.8
% P	0.10	0.03	0.08	0.28	0.53	0.14	0.07
% Ti	0.17	0.27	0.13	0.2	0.38	0.9	0.23
% Mn	0.015	0.002	0.011	0.018	0.03	0.2	0.06
ppm Ba	448	36	340	520	985	300	830
ppm Ce	28	3.2	19	34	64	48	100
ppm Co	6	0.71	5	8	15	200	25
ppm Cr	43	3.3	36	51	97	100	5
ppm Cu	32	6.6	20	56	106	45	14
ppm Ga	9	1.31	5	11	21	18	20
ppm La	14	1.6	10	17	32	17	55
ppm Li	35	3.4	26	40	76	15	40
ppm Mo	9	2.9	5	20	38	2	1.4
ppm Nb	5	0.66	3	6	11	20	24
ppm Nd	13	2.1	9	18	34	20	46
ppm Ni	36	2.2	31	42	80	160	8
ppm Pb	15	2.8	9	23	44	8	20
ppm Sc	6	0.73	5	7	13	24	3
ppm Sr	271	46	170	370	701	440	300
ppm Th	5	1.1	3	7	13	4	18
ppm V	76	4.8	64	87	165	200	40
ppm Y	10	1.0	8	12	23	25	42
ppm Zn	74	8.1	58	92	174	105	50
% C_{org}	3.8	0.443	2.74	4.75			
% N	0.45	0.057	0.26	0.58			
C/N	8.44	0.07	7.6	10.58			
% biopal[c]	30.9	3.55	26.5	34.7			

[a] Nonbiogenic—see text for method of calculation.
[b] Includes Na and Mg from interstitial sea salts because samples were not washed prior to drying.
[c] Top 25 cm only.

contribution of factor 1 has increased considerably over the last 40 years, whereas that of factor 3 has decreased slightly (Fig. 3).

Grouping of samples into factor 2 was influenced mostly by Mo and V (Table 3). We interpret Mo as an indicator of the presence of sulfate reduction in pore waters, because it's concentration in detrital-clastic material of any source is so low (<2 ppm) that it can only come from precipitation as a sulfide under oxygen-deficient conditions (Emerson and Huested, 1991; Piper and Dean, 2002; Lyons et al., 2003). The concentration of Mo in seawater is 5–100 times higher than those of other trace elements known to be deposited under conditions of sulfate reduction (e.g., Cd, V, Cu, Zn, and Ni; Emerson and Huested, 1991; Crusius et al., 1996). Based on this interpretation, it would appear from the stratigraphic distribution of factor 2 loadings and Mo concentration (Fig. 3) that the mid-water column on the slope off the west coast of Mexico at the site of BC06 was more oxygen depleted prior to about 40 years ago, and that oxygenation has been increasing over the last 100 years.

Factor 4 is a carbonate factor with contributions mainly from Ca and Sr (Table 3). The $CaCO_3$ content, as calculated from percent excess Ca, of sediments in BC06 is low (<10%) but doubled between 100 and 80 years ago, and has been increasing in recent years (Fig. 3). It is likely that most of the $CaCO_3$ produced in surface waters is dissolved by metabolic CO_2 released from mineralization of organic matter in oxygen-deficient bottom waters and sediments (e.g., Hales and Emerson, 1997; Wenzhöfer et al., 2001). The recent increases in $CaCO_3$ preservation may be the result of less oxygen-deficient water suggested by the decrease in Mo (factor 2), i.e. there has been less decomposition of organic matter, less metabolic CO_2, and higher pH.

4.1.2. BC50

The composition of sediments in BC50 is dominated by a detrital-clastic fraction as judged by the fact that

Table 3
Correlation coefficients between loadings for factors 1–4 and concentrations of major elements (in weight percent) and trace elements (in parts per million, ppm) in BC06

Element	Factor 1	Factor 2	Factor 3	Factor 4
Al	0.58	−0.39	0.64	0.09
Ca	0.52	−0.64	−0.20	0.83
Fe	0.56	−0.49	0.60	0.00
K	0.36	−0.19	0.66	0.13
Mg	−0.17	0.15	0.53	−0.09
Na	−0.78	0.35	−0.16	0.01
P	−0.01	0.05	0.06	0.04
Ti	0.73	−0.49	0.31	−0.10
Mn	0.67	−0.60	0.41	0.32
Ba	0.20	0.41	0.27	−0.31
Ce	0.26	−0.29	0.70	0.04
Co	0.14	−0.40	0.44	0.03
Cr	0.36	−0.38	0.32	0.01
Cu	−0.19	0.24	0.36	0.03
Ga	0.15	−0.54	0.61	0.21
La	0.46	−0.34	0.62	0.04
Li	0.17	−0.04	0.83	−0.09
Mo	−0.43	0.87	−0.16	−0.62
Nb	0.59	0.25	−0.13	−0.28
Nd	−0.25	−0.40	0.44	0.30
Ni	0.20	0.14	0.16	−0.12
Pb	0.07	−0.11	−0.02	0.23
Sc	0.50	−0.24	0.58	−0.10
Sr	0.63	−0.64	−0.14	0.75
Th	−0.04	−0.10	0.30	0.05
V	−0.49	0.56	0.49	−0.34
Y	0.71	−0.34	0.46	−0.07
Zn	0.19	−0.39	0.55	0.25

Table 4
Correlation coefficients between loadings for factors 1–4 and concentrations of major elements (in weight percent) and trace elements (in parts per million, ppm) in BC50

Element	Factor 1	Factor 2	Factor 3	Factor 4
Al	0.97	0.00	0.56	−0.26
Ca	0.52	0.61	0.62	−0.06
Fe	0.94	−0.09	0.56	−0.11
K	0.95	−0.02	0.43	−0.22
Mg	0.80	−0.05	−0.03	−0.17
Na	0.16	0.23	−0.69	−0.01
P	−0.07	−0.39	−0.01	0.93
Ti	0.95	−0.02	0.53	−0.24
Mn	0.95	0.11	0.51	−0.24
Ba	0.82	−0.34	0.47	−0.20
Ce	0.96	−0.10	0.45	−0.26
Co	0.82	0.08	0.39	−0.19
Cr	0.88	−0.38	0.47	−0.06
Cu	0.64	−0.17	0.01	0.21
Ga	0.86	−0.11	0.32	−0.28
La	0.97	−0.01	0.49	−0.24
Li	0.97	0.00	0.53	−0.30
Mo	−0.65	−0.59	−0.23	0.51
Nb	0.77	0.05	0.44	−0.31
Nd	0.84	−0.11	0.38	−0.31
Ni	0.69	−0.53	0.57	0.20
Pb	0.79	0.07	0.13	−0.37
Sc	0.89	0.04	0.42	−0.22
Sr	0.59	0.56	0.63	−0.04
Th	0.61	−0.15	0.19	−0.32
V	0.29	−0.66	0.48	−0.01
Y	0.93	−0.07	0.54	−0.18
Zn	0.89	−0.15	0.36	0.04

factor 1 accounted for most of the variance in the data, and most elements had high positive correlation coefficients with factor 1 loadings (Table 4). Factor 3 also is a detrital-clastic factor but the compositional differences between factors 3 and 1 are not as distinctive as they are for sediments in BC06. The stratigraphic distributions of factors 1 and 3 loadings and element concentrations (Fig. 4) indicate that the relative contribution of the detrital-clastic fraction in sediments at the site of BC50 has increased over the last 180 years.

Factor 2, like factor 4 in BC06, is a carbonate factor defined by concentrations of Ca and Sr. The stratigraphic distribution of $CaCO_3$ (calculated from excess Ca concentration) in BC50 (Fig. 4) is similar to that in BC06 (Fig. 3) in that it increased between 100 and 80 years ago, but not as dramatically as in BC06. The $CaCO_3$ content decreased during the mid-20th century, but has increased in recent years. Concentrations of both Ca and Sr also contribute substantially to detrital-clastic factors in both cores (Tables 3 and 4) suggesting that at least some of the Ca and Sr reside in one or more noncarbonate minerals, probably Ca-plagioclase feldspar (anorthite). Baba et al. (1991a) found that feldspars in sediments in the northern Gulf had a higher proportion of anorthite than sediments from the southern Gulf. This is consistent with the observation that sediments in BC50 contain a higher Ca concentration (Table 2) than sediments in BC06 (Table 1), and Ca contributed to factors 1 and 3 in BC50 as well as factor 2.

Factor 4 is influenced mainly by several high values of P in sediments deposited about AD 1820 (Fig. 4) with a minor contribution from Mo (Table 4). The concentration of Mo was at a maximum of 20 ppm (Fig. 5) coincident with the maximum in P of almost 0.3% in sediments deposited about AD 1820 (Fig. 4), suggesting that lower bottom-water oxygen concentrations at that time probably contributed to higher phosphate accumulation. The Mo concentration in sediments in BC50 has decreased gradually over the last 170 years to about 6 ppm in the most recent sediments (Fig. 5). Assuming that the Mo concentration is a measure of oxygen depletion in bottom waters and sulfate reduction in the sediments, it would appear that the water column on the northern slope of the Guaymas Basin at the site of BC50, like that on the eastern slope of the Guaymas and Carmen Basins at the site of BC06, has become more oxygenated during the 20th century.

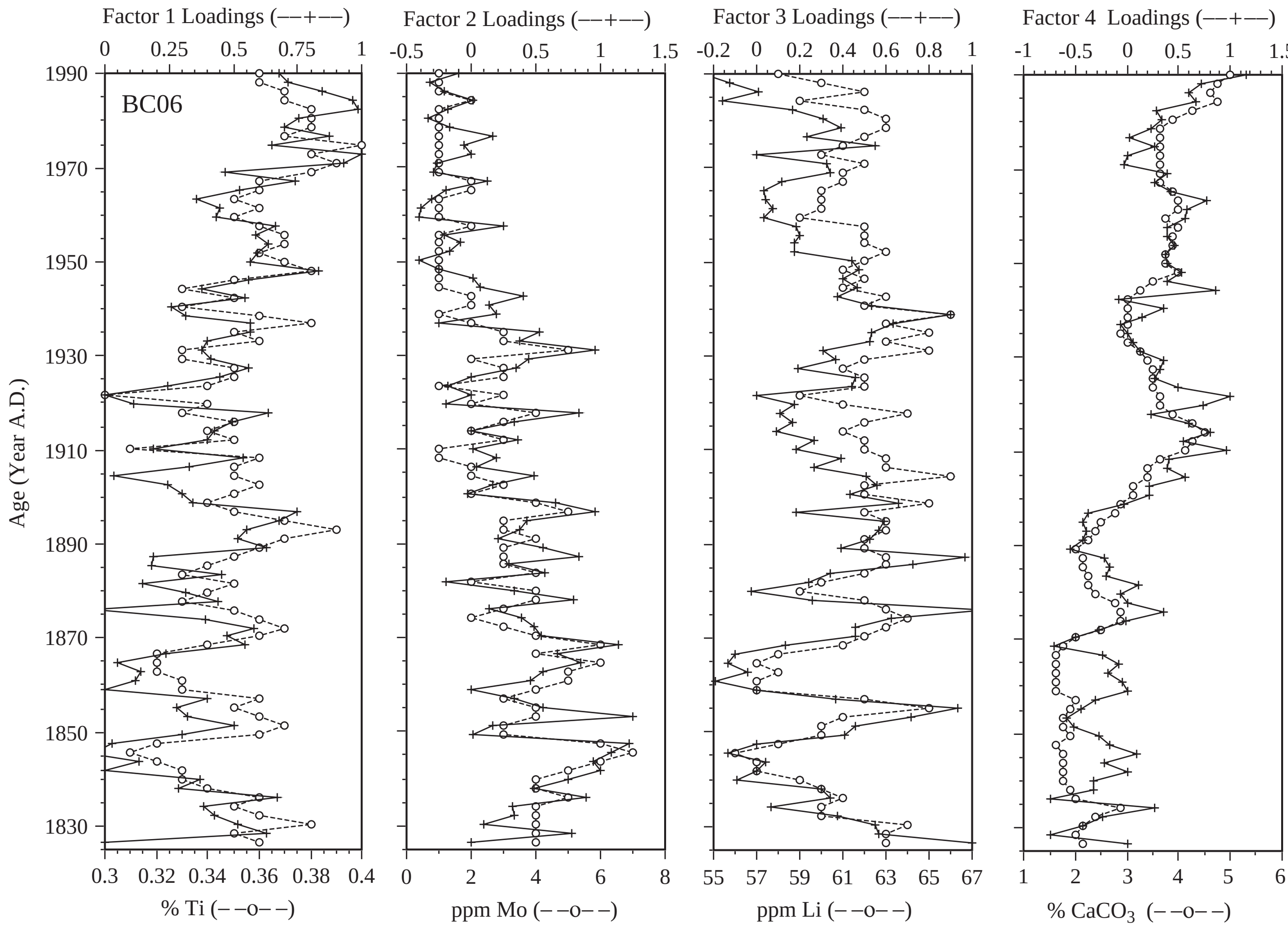

Fig. 3. Profiles of loadings for the four Q-mode factors for sediments from core BC06 versus age in years AD. Also plotted are the concentrations of the element that had a high correlation with the loadings for each factor (dashed lines; Table 3).

4.2. Redox conditions

The Q-mode factor analyses identified redox components in both cores, based mainly on concentrations of Mo and V in BC06, and Mo and P in BC50. In general, there is a negative correlation between the concentration of Mo and concentrations of detrital-clastic components (e.g., factors 1 and 3 elements in BC06; Table 3, Fig. 3) indicating that they are not associated with clastic material.

Because the Gulf of California is a young ocean basin that is still forming, there is a considerable amount of hydrothermal activity, particularly in the Guaymas Basin (Campbell and Gieskes, 1984). As a consequence of this hydrothermal activity, there is a four-fold increase in particulate Mn (presumably as manganese oxyhydroxides) in the water column at depths below the sill in the Guaymas Basin (ca 1500 m) relative to the other basins (Campbell et al., 1988). Because of this, we expected to find relatively high Mn concentrations in the sediments, particularly in BC50. However, concentrations of Mn in sediments in BC50 are actually lower than those in BC06 (Fig. 5), and Mn concentrations in both cores are lower than crustal abundance (ca 0.05%). At water depths of about 750 m, these core sites lie within the range of Pacific intermediate water and are too shallow to be influenced by hydrothermal emissions.

There is a negative correlation between concentrations of Mo and Mn (Table 3, Fig. 5), and this is because these two elements respond oppositely to reducing conditions. Under reducing conditions with sulfate reduction, either in the water column or in sediment pore waters, Mo is precipitated as a sulfide. Iron can exist in sediments in either the oxidized form (e.g., iron oxyhydroxides) or the reduced form (e.g., iron sulfides). However, there are few minerals that contain reduced Mn, the most common being $MnCO_3$ (rhodochrosite). Fig. 5 shows the striking antithetic relations between Mn and Mo in both cores. These relations suggest that over at least the last 180 years, the bottom waters in both basins have become oxygenated with less precipitation of Mo and greater preservation of Mn oxyhydroxides regardless of their source (Landing and Bruland, 1987). Nameroff et al. (2002) examined the

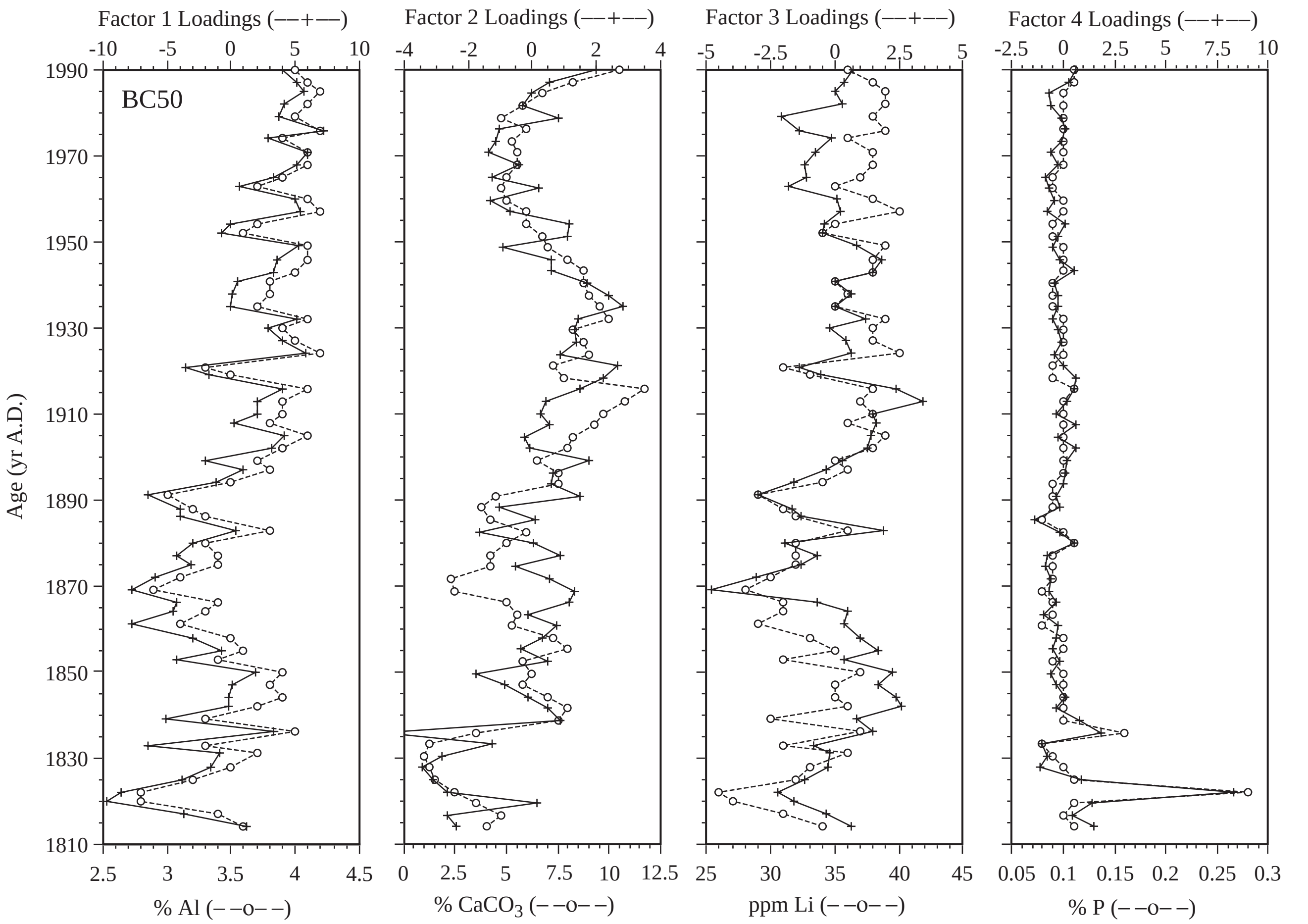

Fig. 4. Profiles of loadings for the four Q-mode factors for sediments from core BC50 versus age in years AD (solid lines). Also plotted are the concentrations of the element that had a high correlation with the loadings for each factor (dashed lines; Table 4).

concentrations of trace elements in sediments in sediment traps and cores on the margin of northwest Mexico off Mazatlan. They found that concentrations of Mn in sediment traps were >1000 ppm ($>0.1\%$) and existed primarily as oxyhydroxides, whereas concentrations in sediments were <300 ppm (0.03%). They concluded that the remineralization of Mn occurs at the sediment–water interface because Mn was not detected in pore waters. In both cores, the concentration of Mo steadily decrease in sediments deposited between AD 1870 and 1950. This suggests that either there was an increase in ventilation of bottom waters in the Gulf, or that the decrease in Mo was related to a decreasing biological oxygen demand on the bottom water, and, therefore, less oxygen deficiency in the water column. Decreased Mo concentration in sediments is particularly striking at the site of BC06 during the last half of the 20th century (Fig. 5). Recent increased ventilation is in line with the observations of De Diego and Douglas (1999) that recent sediments on the open slope off Santa Rosalia on the Baja peninsula (Fig. 1) and in the silled Alfonso Basin off La Paz (Fig. 1) are bioturbated, but rest on undisturbed laminated sediments. The age of the laminated/bioturbated boundary in different cores ranges from 20 to 50 years ago. Schrader and Baumgartner (1983) attributed recent increased oxygenation of bottom waters of the Gulf to a decline in productivity, and, therefore, a lower biological oxygen demand. A decrease in productivity in the Gulf from several hundred years ago to the present was also proposed by DeMaster and Turekian (1987) to explain a decrease in $^{14}C/^{12}C$ in a core from the eastern flank of the Carmen Basin.

4.3. Organic productivity and terrigenous influx

The evidence seems to indicate that the increase in oxygenation of bottom waters in the Gulf was due to decreased organic productivity and a lower biological oxygen demand. The percentage of C_{org} in sediments is often used as a geochemical proxy for organic productivity but because of the potential for differential dilution by terrigenous detritus and other biogenic components, the MAR of C_{org} probably is a better measure of the rate of preservation of organic matter on the bottom at any particular site (Gardner et al., 1997).

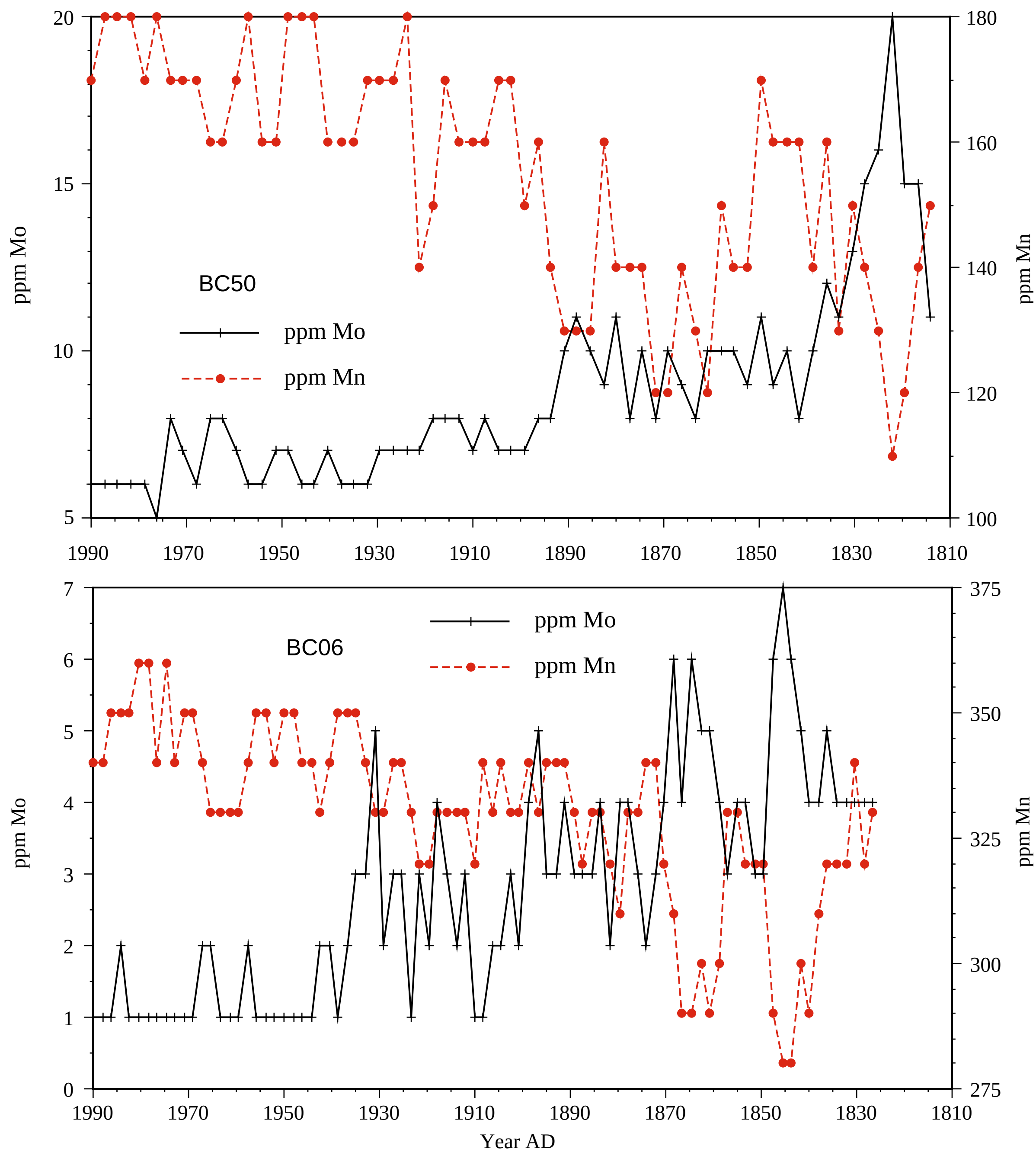

Fig. 5. Plots of ppm Mn (dashed lines) and ppm Mo (solid lines) versus age in years AD for cores BC50 and BC06.

The MARs of C_{org} (as a measure of productivity), aluminum (as a measure of terrigenous detrital flux), and $CaCO_3$ are shown for cores BC06 and BC50 in Fig. 6. Unfortunately, we do not have down-core variations in the MAR of biopal, the other major biogenic component in Gulf of California sediments. The fluxes of all three components appear to increase over the last 170 years in BC06 (Fig. 6). Actually, the MAR of C_{org} fluctuates considerably, but does not really change until about AD 1950 when it increases slightly. This could be interpreted as an increase in productivity, which would go against the suggestion of Schrader and Baumgartner (1983) of decreased productivity. More likely, the downward decrease in C_{org} MAR in both cores from the top of the core to sediments deposited during the mid-20th century is due to burial diagenesis or ‘‘burndown’’ of freshly deposited labile organic matter (e.g., Tromp et al., 1995; Canuel and Martens, 1996; Dean and Gardner, 1998). The mixture of organic matter that has been buried in the anoxic sediments below the depth of diagenesis consists of refractory organic matter and labile organic matter that escaped burndown.

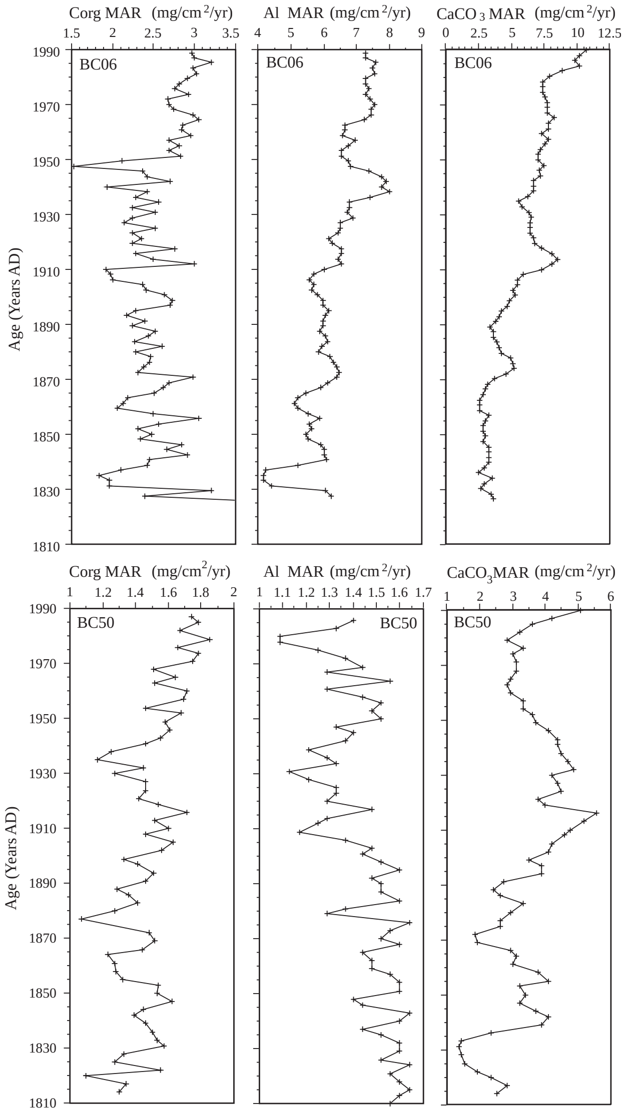

Fig. 6. Plots of MARs of C_{org}, Al, and $CaCO_3$ in years AD for cores BC50 and BC06.

The increase in Al MAR in BC06 indicates that the detrital-clastic influx to the site of BC06 increased over the last 170 years, probably due to land clearing and increased sediment loads to the rivers draining the Sierra Madre. Dam construction on these rivers during the last half of the 20th century apparently did not greatly affect sediment supply reaching the site of BC06. Baba et al. (1991b) observed no consistent changes in the accumulation rate of terrigenous sediment in the Guaymas Basin over the last century. They attributed this to a constant supply of eolian material from the mainland as suggested by Baumgartner et al. (1991). However, it could also be due to resuspension of fine-grained sediment from the shelf. The $CaCO_3$ MAR also increased slightly, perhaps reflecting increased productivity of calcareous nanoplankton as diatom and silicoflagellate productivity decreased, as suggested Schrader and Baumgartner (1983), and/or decreased dissolution of $CaCO_3$ in oxygen-deficient bottom waters. The bulk-sediment MAR reflects the sum total of the MARs of all of the sediment components. The bulk-sediment MAR in core BC06 increased from 60 to more than 100 mg/cm^2/yr over the 170-year period of record. This suggests that the damming of rivers in the Sierra Madre during the second half of the 20th century had little effect on detrital-clastic sedimentation at the site of BC06.

Although, % Al in BC50 increased over the 180-year period of record (Fig. 4), the Al MAR decreased (Fig. 6). This decrease in detrital-clastic material probably reflects the decrease in delivery of water and sediment to the northern Gulf of California by the Colorado River as dams were built and more and more water was removed for municipal and agricultural uses. Today the Colorado River rarely reaches the Gulf of California.

As discussed above, we believe that the increase in C_{org} MAR in the last half of the 20th century in both cores is due to the incomplete burndown of labile organic matter. The increase of C_{org} MAR also could be due to influx of more terrestrial organic matter during the 20th century; however, the organic matter in the sediments in both cores is predominantly marine, as indicated by C/N ratios of 6–10 (Tables 1, 2 and 5). This is true for organic matter in the Gulf in general based on organic geochemical analyses of sediments in Deep Sea Drilling Project (DSDP) cores (Simoneit, 1991). The isotopic evidence also suggests that the organic matter is predominantly marine. Values of $\delta^{13}C$ and $\delta^{15}N$ of sediments in the tops of eight box cores average −21.0‰ and 10.3‰, respectively, with very little variation (Table 5; Pride et al., 1999). Values of $\delta^{13}C$ in sediment-trap samples average −20.6‰, again, with very little variation (Thunell, 1998). Such values are typical of planktonic marine organic matter (Peters et al., 1978; Emerson and Hedges, 1988; Dean and Gardner, 1998).

Diatoms are the main contributors to the flux of C_{org} in the Gulf of California (e.g., Schrader and Baumgartner, 1983; Sancetta, 1995). Sediment-trap studies by Thunell (1998) showed that although there was a strong seasonal pattern in the flux of biopal in the Gulf, there is little seasonal variation in the flux of organic carbon. He concluded that carbon flux does not appear to be as reliable a proxy for primary productivity as does biopal flux. The limited biopal data we have show that the biopal content in surface sediments in BC50 (Table 2) is considerably higher that for those in BC06 (Table 1). The depth distributions of those limited samples (not shown) suggest that biopal contents decreased in sediments deposited in the 20th century, which is supported by the observed lower productivity based on silicoflagellate populations and abundance of benthic foraminifera (Schrader and Baumgartner, 1983; Barron

Table 5
Carbon and nitrogen isotopic compositions, and C/N ratios of organic matter, in samples of sediment from the tops of eight box cores

Box core	Depth (cm)	$\delta^{13}C_{org}$	$\delta^{15}N$	C/N
6	0.5	−21.15	9.70	9.74
6	1.5	−20.95	9.79	9.66
6	2.25	−20.81	9.68	9.77
6	2.5	−21.03	10.02	10.04
6	3.25	−20.66	9.37	9.27
6	4.25	−20.67	9.90	9.02
6	5.25	−20.60	9.84	9.21
10	0.25	−20.62	10.38	8.35
10	1.25	−20.88	10.26	8.81
10	2.25	−23.17	10.13	9.06
10	3.25	−20.68	10.16	9.33
10	4.25	−20.84	9.95	8.43
10	6.25	−21.16	10.44	9.16
10	7.25	−21.00	10.08	9.04
21	0.25	−20.76	10.30	
21	1.25	−20.88	10.49	
21	22.5	−20.87	10.04	
21	3.25	−20.84	10.44	
33	0.25	−20.95		
33	1.25	−21.67	9.77	8.88
33	2.25	−21.73	10.10	8.73
33	3.25	−21.84	10.79	9.07
33	4.25	−20.74	10.44	9.7
33	5.25	−19.83	10.80	8.9
35	0.25	−21.68	10.59	9.57
35	1.25	−21.53		
35	2.25	−21.77	9.76	9.70
35	3.25	−23.38	9.69	9.31
35	4.25	−20.49	10.34	9.43
35	5.25	−20.47	10.32	9.43
43	0.25	−21.84	11.04	
43	0.75	−21.55		
43	1.75	−21.91	11.58	
43	2.25	−21.30	10.92	
43	3.25	−21.25	11.71	
50	0.3	−21.10	10.35	
50	0.5	−20.99	9.95	9.64
50	1.3	−20.82	10.14	9.83
50	1.5	−21.09		10.17
50	2.3	−21.24	10.41	9.55
50	2.9	−20.78	10.05	9.75
50	3.1	−21.08	10.12	9.85
50	3.7	−20.77	10.02	9.86
57	0.25	−19.97	10.19	7.63
57	1.25	−19.97	10.39	7.67
57	2.25	−20.10	10.22	7.82
57	3.25	−20.00	10.43	7.91
57	4.25	−20.30	10.52	8.94
57	5.25	−20.33	10.28	7.92

et al., 2003) and silica oxygen isotopes (Julliet-Leclerc and Schrader, 1987).

4.4. Cyclicity

Because the Gulf of California has such a distinct annual cycle of circulation, precipitation, upwelling, and productivity, and because that region of the Pacific Ocean is sensitive to interannual (ENSO) and decadal (PDO) climatic variations, we would expect that the sediment of the Gulf would have distinct cyclicities in the delivery of sediment components, as demonstrated by the annual varve components (Calvert, 1966; Baumgartner et al., 1991) and sediment-trap studies (Thunell, 1998). Cyclicity is indeed a distinct characteristic of the sediments of the Gulf of California, ranging in periodicity from the annual varve laminations to decadal, centennial-, and millennial-scale fluctuations in sediment components. Schrader and Baumgartner (1983) constructed a productivity index based on changes in silicoflagellate populations. Using this index, they identified six periods of increased productivity between AD 1450 and 1950 with an average periodicity of about 100 years. Barron et al. (2003) used percent biogenic silica as a proxy for diatom productivity, and found that diatom productivity in the Gulf increased about every 200 years, roughly coincident with minima in solar activity as inferred from cycles in radiocarbon production (the so-called Suess cycles; Damon and Sonett, 1991). They suggested that solar minima result in atmospheric cooling above northwest Mexico increasing the strength of northwesterly winds that produce upwelling in the Gulf. Douglas et al. (2002) constructed a gray-scale varve-thickness time series for varved sediments in cores from the Alfonso Basin, a closed depression in La Paz Bay on the southeastern coast of Baja. Spectral analyses of the varve-thickness time series revealed a dominant periodicity of 200–300 years. Another prominent periodicity was 14–41 years, which corresponds to dark-light banding in the cores. Other periodicities of 4–6 and 7–13 years were suggestive of timing of ENSO events and sun-spot variations.

Many geochemical components in both BC06 and BC50 exhibit a distinct cyclicity with periodicities of 10–20 years. This can be seen in some of the plots of element concentrations and factor loadings in Figs. 3 and 4, particularly for the detrital-clastic factors 1 and 3 in BC06. We were particularly impressed with the striking cycles in Ti (Fig. 4) as well as Y, Mn, Nb, Al, and Fe, the other factor 1 elements in core BC06, with periodicities of about 10–20 years. We thought that these decadal cycles might coincide with the 11-year sun-spot cycle or the so-called "double sun-spot cycle" that is also known from solar activity (e.g., Damon and Sonett, 1991; Lean and Rind, 1998). However, Biondi et al. (2001) concluded that the internal dynamics of the coupled ocean-atmosphere system in the northeastern Pacific, as expressed by the PDO, had a greater influence on Pacific climate than solar forcing. The PDO is an expression of cold-season (October–March) sea-surface temperature variability (Mantua et al., 1997). Biondi et al. (2001) reconstructed a PDO index since AD 1660 based on tree rings (http://www.ngdcd.noaa.gov/paleo/

pubs/biondi2001/biondi2002.html). During warm PDO intervals, the eastern Pacific experiences stronger Aleutian Lows, and is warmer than usual with higher winter precipitation (e.g., Biondi et al., 2001; Gedalof et al., 2002). The opposite is true during cool PDO intervals. Biondi et al. (2001) used tree-ring records for Jeffrey pine (*Pinus jeffreyi*) and Douglas fir (*Pseudotsuga macrocarpa*) from the coasts of Southern California and Baja California. These species are mostly influenced by cool-season precipitation variability and should be a good proxy for precipitation in the region affecting the Gulf of California.

We then looked at winter precipitation over the last two centuries, as interpreted from the reconstructed PDO index (Biondi et al., 2001), compared with our Ti data (Fig. 7). Our reasoning was that concentrations of Ti are much higher in mafic volcanic rocks than in more felsic rocks (Tables 1 and 2), and the Sierra Madre is large pile of volcanic rocks. Core BC06 was collected just off shore from two of the largest rivers draining the Sierra Madre, Rio Yaqui, and Rio Mayo (Fig. 1). Although, dams were constructed on these rivers during the latter part of the 20th century, apparently this did not significantly reduce the sedimentation rate at the site of BC06 because the ^{210}Pb decay curves for both cores are remarkably linear with depth (Thunell et al., 1994), and the accumulation rate of detrital-clastic material was not affected. Periods of increased precipitation (warm phases of PDO with more El Niños) should be matched by enhanced runoff and delivery of Ti-rich volcanic debris to the Gulf. Dry periods (cool phases of PDO with more La Niñas) should be matched with decreased run off and delivery of Ti-rich sediments. Fig. 7 shows that the agreement between winter rainfall (PDO index) and delivery of detrital volcanic debris (% Ti) is very good, particularly for the 19th century, considering the limitations on dating of the two records. Warm phases of PDO and greater delivery of volcanic debris occurred at about AD 1830, 1850, 1870, and 1890 (Fig. 8).

To more objectively examine the cycles in the geochemical data, which appear to be best developed in the sediments in core BC06, we applied wavelet analysis (Prokoph and Barthelmes, 1996; Torrence and Campo, 1998) that computes a type of evolutionary power spectrum, i.e., one that computes variation in spectral power at different periodicities with time. Wavelet analysis is particularly useful for analyzing cycle periodicities in nonstationary data, i.e., data that may contain periodic signals that may vary in both frequency and amplitude with time. Such data (most geologic data) limit the interpretation of a single power spectrum for an entire time series. We used the two-dimensional Gaussian wavelet, the so-called ''Mexican hat'' wavelet, that is particularly useful for analyzing ''noisy'' nonstationary data (Prokoph and Barthelmes, 1996).

We first applied wavelet analysis to the Ti data for core BC06 (Fig. 8) and the PDO index (Fig. 9) for the last 170 years. The wavelet analyses for Ti (Fig. 8) show significant power in the bidecadal (16–32 years) periodicity band and in the multidecadal (>32 years) band. The multidecadal periodicity occurs throughout the 170-year time series, but the bidecadal periodicity has the highest power for sediments deposited prior to AD 1900.

The wavelet analyses for Ti (Fig. 8) also show some power in the 4–8- and 8–16-year periodicity bands in sediments deposited between AD 1910 and 1950), suggesting that there might be an ENSO forcing. Although, these sediments were deposited in the 20th century, they were deposited before major dam construction on the rivers draining the Sierra Madre.

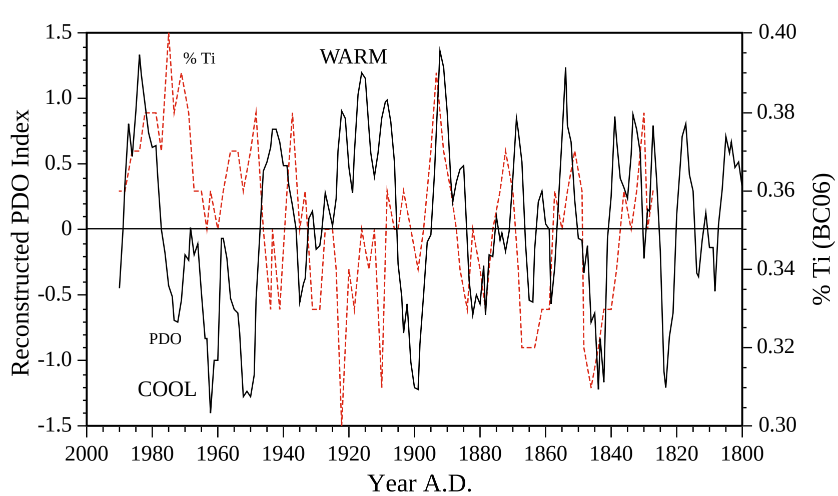

Fig. 7. Plots of the PDO index (solid line) reconstructed from tree rings (Biondi et al., 2001), and % Ti in core BC06 (dashed line) versus age in years AD.

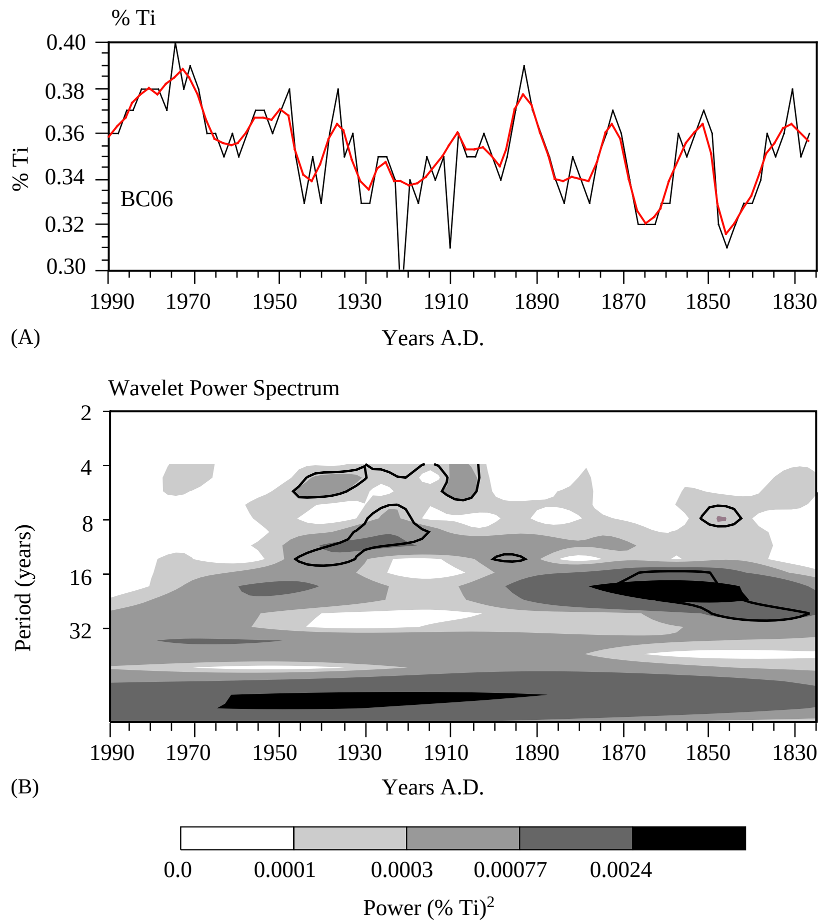

Fig. 8. (A) Plot of % Ti in sediments from core BC06 versus age in years AD. The heavy curve through the data is a weighted smoothing function. (B) Wavelet power spectrum of % Ti. The shaded contour intervals are chosen so that 75%, 50%, 25%, and 5% of the wavelet power is above each level, respectively.

The wavelet analyses of the PDO index (Fig. 9) also show significant power in the bidecadal (16–32 years) periodicity band and in the multidecadal (>32 years) band. The multidecadal periodicity has the highest power during the 20th century, whereas the bidecadal periodicity has the highest power during the last half of the 19th century and the first half of the 20th century. The multidecadal periodicity can be seen in the raw data (Figs. 7 and 9A) as longer durations of warm and cool phases of the PDO.

In summary, we are somewhat hesitant to interpret the geochemical data in terms of depositional conditions and climate for sediments deposited during the 20th century because of damming of rivers. However, it appears that the sediments deposited in the 19th century do exhibit distinct 20-year periodicities in geochemical variables reflecting redox conditions (molybdenum) as well as detrital influx. The next step is to determine if these cycles extend farther back in time. There is also spectral evidence for periodicities of 4–8 and 8–16 years suggesting that the delivery of detrital-clastic material is responding to some multiannual (ENSO?) forcing.

5. Conclusions

Q-mode factor analyses of elemental geochemical data in sediments deposited over the last 180 years collected in two box cores on the slopes of the Guaymas and Carmen Basins in the central Gulf of California identified detrital-clastic, carbonate, and redox associations. Box core BC06 was collected in a water depth of 754 m close to the west coast of mainland Mexico between the mouths of two of the largest rivers draining the Sierra Madre Occidental, Rio Yaqui, and Rio Mayo. The dominant sediment component in BC06 is a detrital-clastic fraction, probably mafic volcanic debris from the Sierra Madre because of high concentrations of Ti, Mn, and Fe. A second detrital-clastic association was identified in BC06 with relatively high concentrations of Li, Ce, K, and Al, suggesting that it was derived from a more felsic source, probably the Colorado Plateau via the Colorado River. The contribution of the more mafic clastic component has increased considerably over the last 40 years, whereas the more felsic contribution has decreased, again suggesting a Colorado River source

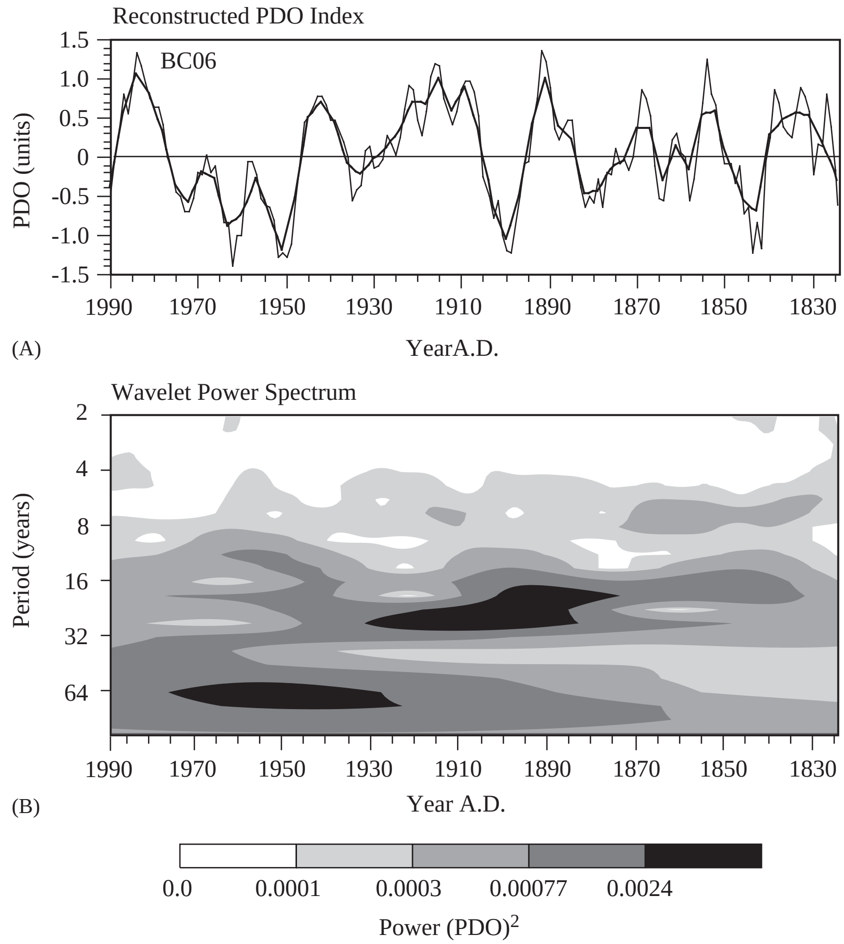

Fig. 9. (A) Plot of reconstructed PDO index versus age in years AD. The heavy curve through the data is a weighted smoothing function. (B) Wavelet power spectrum of PDO. The shaded contour intervals are chosen so that 75%, 50%, 25%, and 5% of the wavelet power is above each level, respectively.

because today the Colorado River rarely reaches the Gulf of California.

A redox association in BC06 is based on relatively high concentrations of Mo and V, both indicative of deposition under conditions of sulfate reduction. Decreases in concentrations of these elements in younger sediments suggest that oxygenation of the mid-water column on the slope off the west coast of Mexico has been increasing over the last 100 years.

Box core BC50 was collected on the northern slope of the Guaymas Basin in a water depth of 745 m. The sediments in this core are more biogenic than those in BC06, with higher concentrations of biogenic silica. Most inorganic elements in sediments from BC50 are associated with a detrital-clastic component that is more felsic in composition than the dominant detrital component in BC06, probably reflecting its location closer to the delta of the Colorado River. The mass accumulation rate of the detrital-clastic fraction (Al MAR) has decreased over the last 180 years reflecting the decrease in delivery of water and sediment from the Colorado River. A redox association in sediments from BC50, based mainly on the concentration Mo, suggests that the water column at the site of BC50, like that at the site of BC06, has become more oxygenated over the last 100–170 years. Increased oxygenation in bottom waters of the Gulf in recent years probably is due to a decrease in biological oxygen demand resulting from decreasing productivity.

Many geochemical components in both BC06 and BC50 exhibit a distinct cyclicity with periodicities of 10–20 years. The most striking are 20-year cycles in the volcanoclastic elements (e.g., Ti) in sediments in core BC06 deposited during the 19th century. A wavelet spectral analysis of the Ti data for BC06 shows significant power in the bidecadal (16–32 years) periodicity band and in the multidecadal (>32 years) band. The wavelet analyses for Ti also show some power in the 4–8- and 8–16-year periodicity bands in sediments deposited between AD 1910 and 1950, suggesting that there might be an ENSO forcing.

Using a reconstructed PDO index as a measure of winter precipitation, there is a very good agreement between cycles in PDO index and cycles in Ti-rich

volcanic debris, particularly in the 19th century. The cycles are interpreted as wet–dry cycles corresponding to periods of increased–decreased delivery of volcanic detritus from the Sierra Madre Occidental.

Acknowledgements

The paper benefited greatly from thoughtful comments by two anonymous reviewers. We thank John Barron and Michele Tuttle for critical comments on an earlier draft of this paper. Funding for W.D. was provided by the USGS Global Change and Climate History, and Earth Surface Dynamics Programs.

References

Baba, J., Peterson, C.D., Schrader, H.J., 1991a. Modern fine-grained sediments in the Gulf of California. In: Dauphin, J.P., Simoneit, B.R.T. (Eds.), The Gulf and Peninsular Province of the Californias. American Association of Petroleum Geologists Memoir 47, 569–587.

Baba, J., Peterson, C.D., Schrader, H.J., 1991b. Fine-grained terrigenous sediment supply and dispersal in the Gulf of California during the last century. In: Dauphin, J.P., Simoneit, B.R.T. (Eds.), The Gulf and Peninsular Province of the Californias. American Association of Petroleum Geologists Memoir 47, 589–602.

Barron, J.A., Bukry, D., Bischoff, J.L., 2003. A 2000-yr-long record of climate from the Gulf of California. In: West, G.J., Buffaloe, L.D. (Eds.), Proceedings of the 19th Pacific Climate Workshop. Asilomar, Pacific Grove, CA, 2002, pp. 11–21.

Baumgartner, T.R., Ferreira-Bartrina, V., Moreno-Hentz, P., 1991. Varve formation in the central Gulf of California: a reconsideration of the origin of the dark laminae from the 20th century varve record. In: Dauphin, J.P., Simoneit, B.R.T. (Eds.), The Gulf and Peninsular Province of the Californias. American Association of Petroleum Geologists Memoir 47, 617–635.

Biondi, F., Gershunov, A., Cayan, D.R., 2001. North Pacific decadal climate variability since 1661. Journal of Climate 14, 5–10.

Bray, N.A., 1988. Watermass formation in the Gulf of California. Journal of Geophysical Research 93, 9223–9240.

Briggs, P.H., 2002. The determination of forty elements in geological and botanical samples by inductively coupled plasma-atomic emission spectrometry. In: Taggart, J.E., (Ed.), Analytical Methods for Chemical Analyses of Geologic and other Materials. US Geological Survey Open-File Report 02-223, pp. G1–20.

Calvert, S.E., 1966. Origin of diatom-rich, varved sediments from the Gulf of California. Journal of Geology 76, 546–565.

Campbell, A.C., Gieskes, J.M., 1984. Water column anomalies associated with hydrothermal activity in the Guaymas Basin, Gulf of California. Earth and Planetary Science Letters 68, 57–72.

Campbell, A.C., Gieskes, J.M., Lupton, J.E., Lonsdale, P.F., 1988. Manganese geochemistry in the Guaymas Basin, Gulf of California. Geochimica et Cosmochimica Acta 52, 345–357.

Canuel, E.A., Martens, C.S., 1996. Reactivity of recently deposited organic matter: degradation of lipid compounds near the sediment–water interface. Geochimica et Cosmochimica Acta 60, 1793–1806.

Crusius, J., Calvert, S., Pedersen, T., Sage, D., 1996. Rhenium and molybdenum enrichments in sediments as indicators of oxic, suboxic, and sulfidic conditions of deposition. Earth and Planetary Science Letters 145, 65–78.

Damon, P.E., Sonett, C.P., 1991. Solar and terrestrial components of the atmospheric ^{14}C variation spectrum. In: Sonett, C.P., Giampapa, M.S., Matthews, M.S. (Eds.), The Sun in Time. The University of Arizona Press, Tucson, AZ, pp. 360–388.

Dean, W.E., Gardner, J.V., 1998. Pleistocene to Holocene contrasts in organic matter production and preservation on the California continental margin. Geological Society of America Bulletin 110, 888–899.

De Diego, T., Douglas, R.G., 1999. Oxygen-related sediment microfabrics in modern "black shales", Gulf of California, Mexico. Journal of Foraminiferal Research 29, 456–464.

DeMaster, D.J., Turekian, K.K., 1987. The radiocarbon record in varved sediments of Carmen Basin, Gulf of California: a measure of upwelling intensity variation during the past several hundred years. Paleoceanography 2, 249–254.

Douglas, R.G., Gorsline, D., Grippo, A., Granados, I., Gonzalez-Yajimovich, O., 2002. Holocene ocean-climate variations in Alfonso Basin, Gulf of California, Mexico. In: West, G.J., Buffaloe, L.D. (Eds.), Proceedings of the 18th Pacific Climate Workshop. Asilomar, Pacific Grove, CA, 2002, pp. 7–20.

Emerson, S.R., Hedges, J.I., 1988. Processes controlling the organic carbon content of open ocean sediments. Paleoceanography 3, 621–634.

Emerson, S.R., Huested, S.S., 1991. Ocean anoxia and concentrations of molybdenum and vanadium in seawater. Marine Chemistry 34, 177–196.

Gardner, J.V., Dean, W.E., Dartnell, P., 1997. Biogenic sedimentation beneath the California Current system for the past 30 ky and its paleoceanographic significance. Paleoceanography 12, 207–225.

Gedalof, Z., Mantua, N.J., Peterson, D.L., 2002. A multi-century perspective of variability in the Pacific Decadal Oscillation: new insights from tree rings and coral. Geophysical Research Letters 29, 2204 (doi:10.1029/2002GLo15824).

Hales, B., Emerson, S., 1997. Evidence in support of first-order dissolution kinetics of calcite in seawater. Earth and Planetary Science Letters 148, 317–327.

Julliet-Leclerc, A., Schrader, H., 1987. Variation in upwelling intensity recorded in varved sediment from the Gulf of California during the past 3000 years. Nature 329, 146–149.

Klovan, E., Miesch, A.T., 1976. Extended CABFAC and QMODEL computer programs for Q-mode factor analysis of compositional data. Computers and Geosciences 1, 161–178.

Krauskopf, C.B., 1967. Introduction to Geochemistry. McGraw-Hill, New York, 721pp.

Kuehl, S.A., Fugelseth, T.J., Thunell, R.C., 1993. Sediment mixing and accumulation rates in the Sulu and South China Seas: implications for organic carbon preservation in deep-sea environments. Marine Geology 11, 15–35.

Landing, W.M., Bruland, K.W., 1987. The contrasting biochemistry of iron and manganese in the Pacific Ocean. Geochimica et Cosmochimica Acta 51, 29–43.

Lean, J., Rind, D., 1998. Climate forcing by changing solar radiation. Journal of Climate 11, 3069–3094.

Lyons, T.W., Werne, J.P., Hollander, D.J., Murray, R.W., 2003. Contrasting sulfur geochemistry and Fe/Al and Mo/Al ratios across the last oxic-to-anoxic transition in the Cariaco Basin, Venezuela. Chemical Geology 195, 131–137.

Mantua, N.J., Hare, S.R., Zhang, Y., Wallace, J.M., Francis, R.C., 1997. A Pacific interdecadal climate oscillation with impacts on salmon production. Bulletin of the American Meteorological Society 78, 1069–1079.

Moore, D.G., 1973. Plate-edge deformation and crustal growth, Gulf of California structural province. Geological Society of America Bulletin 84, 1883–1906.

Mortlock, R.A., Froelich, P.N., 1989. A simple method for the rapid determination of biogenic opal in pelagic marine sediments. Deep-Sea Research 36, 1415–1426.

Nameroff, T.J., Balistrieri, L.S., Murray, J.W., 2002. Suboxic trace metal geochemistry in the eastern tropical North Pacific. Geochemica et Cosmochimica Acta 66, 1139–1158.

Parker, R.L., 1967. Data of Geochemistry. Composition of the Earth's Crust. US Government Printing Office, Washington, 19pp (Chapter D).

Peters, K.E., Sweeney, R.E., Kaplan, I.R., 1978. Correlation of carbon and nitrogen stable isotope ratios in sedimentary organic matter. Limnology and Oceanography 23, 598–604.

Pike, J., Kemp, A.E.S., 1997. Early Holocene decadal-scale ocean variability recorded in Gulf of California laminated sediments. Paleoceanography 12, 227–238.

Piper, D.Z., Dean, W.E., 2002. Trace-element deposition in the Cariaco Basin under sulfate reducing conditions—a history of the local hydrography and global climate, 20 ka to the present. US Geological Survey Prof. Paper 1670, 41pp.

Pride, C., Thunell, R., Sigman, D., Keigwin, L., Altabet, M., Tappa, E., 1999. Nitrogen isotopic variations in the Gulf of California since the last deglaciation. Response to global climate change. Paleoceanography 14, 397–409.

Prokoph, A., Barthelmes, F., 1996. Detection of nonstationarities in geological time series: wavelet transform of chaotic and cyclic sequences. Computers and Geosciences 22, 1097–1108.

Sancetta, C., 1995. Diatoms in the Gulf of California: seasonal flux patterns and the sediment record for the last 15,000 years. Paleoceanography 10, 67–84.

Schrader, H., Baumgartner, T., 1983. Decadal variation of upwelling in the central Gulf of California. In: Thiede, J., Suess, E. (Eds.), Coastal Upwelling, its Sediment Record, Part B: Sedimentary Records of Ancient Coastal Upwelling. Plenum Press, New York, pp. 247–276.

Simoneit, B.R.T., 1991. Organic geochemistry of Deep Sea Drilling Project cores from Legs 63 to 66—a synthesis of sources, preservation, and maturity of organic matter in Quaternary and Neogene sediments from an active continental margin. In: Dauphin, J.P., Simoneit, B.R.T. (Eds.), The Gulf and Peninsular Province of the Californias. American Association of Petroleum Geologists Memoir 47, 667–703.

Thunell, R.C., 1998. Seasonal and annual variability in particle fluxes in the Gulf of California: a response to climate forcing. Deep-Sea Research I 45, 2059–2083.

Thunell, R.C., Pride, C.J., Tappa, E., Muller-Karger, F.E., 1994. Biogenic silica fluxes and accumulation rates in the Gulf of California. Geology 22, 303–306.

Torrence, C., Campo, G.P., 1998. A practical guide to wavelet analysis. Bulletin of the American Meteorological Society 79, 61–78.

Tromp, T.K., Van Cappellen, P., Key, R.M., 1995. A global model of the early diagenesis of organic carbon and organic phosphorus in marine sediments. Geochimica et Cosmochimica Acta 59, 1259–1284.

Wedepohl, K.H., 1995. The composition of the continental crust. Geochimica et Cosmochimica Acta 59, 1217–1232.

Wenzhöfer, F., Adler, M., Kohls, O., Hensen, C., Strotmann, B., Boehme, S., Schulz, H.D., 2001. Calcite dissolution driven by benthic mineralization in the deep-sea: in situ measurements of Ca^{2+}, pH, pCO_2, and O_2. Geochimica et Cosmochimica Acta 65, 2677–2690.